Journal of Optoelectronics and Advanced Materials Vol. 5, March 2003, p. 293 - 300

MODELING THE MULTI-CRYSTALLINE SILICON INGOT SOLIDIFICATION PROCESS IN A VERTICAL SQUARE FURNACE

F. Barvinschi*, C. Stelian[a], Y. Delannoy[b], N. Mangelinck[b], T. Duffar[b]

"Politehnica" Univ. of Timisoara, Dept. of Physics, Regina Maria, 1, 1900 Timisoara, Romania
[a]Dept. of Physics, West University of Timisoara, Bd. V. Parvan, No. 4, 1900 Timisoara, Romania
[b]EPM, ENSHMG, BP-95, 38402, St. Martin d'Héres, France

Large-scale production of multi-crystalline silicon for high-efficient solar cells is a very important task of today's photovoltaic technology. The efficiency of crystalline silicon solar cells depends on both the crystallization process and the solar cell processing sequence. As far as the crystallization process is concerned, it is very important to know the temperature distribution during the solidification of silicon ingots, to predict the solidification structure obtained and thus the materials properties. In this study the transient 2D and stationary 3D numerical simulation of the solidification process of large square mc-Si ingots is investigated, by using the software FIDAP and Fluent™. Some geometrical approximations of the real furnace and specific approaches for the radiation modelling are used in order to solve the difficulties related to numerical analysis. The results are compared to the experimental data, in order to calibrate the numerical model.

(Received July 20, 2002, in revised form March 6, 2003;
accepted after revision March 12, 2003)

Keywords: Multi-crystalline silicon, Radiative heat transfer, Numerical simulation

1. Introduction

High quality large-scale ingots of poly-crystalline silicon, used for the solar cell production, can be obtained when the thermal environment surrounding the casting charge is precisely controlled [1]. Optimum growth conditions are explored efficiently by numerical simulation of the main physical phenomena and processing conditions, the results being useful for an improved design of the mc-Si industrial device. Since the basic physical laws known, modelling procedures for solving their differential equations may be considered as a substitute of the experiment, and may be used, on the engineering point of view, to help the improvement of the existing set-up.

The basic principle for producing up to 200 Kg mc-Si ingots [2] consists of melting and then solidifying the charge in a controlled direction, from the bottom upwards, to obtain a large-grain poly-crystalline structure. Defects acting on the solar cell performances are [3] (i) the concentration and type of impurity atoms, (ii) the electrical activity of extended defects and grain boundaries and (iii) the interactions of impurity atoms (complex and cluster formation) as relevant parameters.

In a first approach, presented in the second paragraph, the 2D transient modelling of the solidification process using FIDAP® is realised. In the third paragraph of this work, the 3D steady state modelling of the heat transfer during the formation of these ingots is investigated, by using the

* Corresponding author: fbarvinschi@etv.utt.ro

expertise we have in the field of large industrial plants [4-6]. The somewhat complicated problem of coupled heat transport by conduction and by radiation is studied with the software Fluent™ [7].

2. 2D transient modelling

2.1. Model and mathematics

Due to the high number of nodes and computational limitations, a 2D geometrical model is used for the transient simulation. The grid generator GAMBIT® has been used to create a paved mesh with about 12000 quadrilateral elements. The density of nodes is increased in the silicon sample for a better computation of the thermal field.

The heat transfer by conduction, convection and radiation is calculated by using the code FIDAP®. Because of the low value of the Prandtl number of silicon, the effect of the melt convection on the thermal field can be neglected. Furthermore, the small value of temperature gradient on the vertical axis of the installation indicates that the intensity of the buoyancy melt convection is low. So, the melt convection has been neglected in our simulation.

The heat transfer equation, which determines the temperature distribution in the furnace, is:

$$\rho c_P \frac{\partial T}{\partial t} = k\nabla^2 T \tag{1}$$

where ρ, c_P and k are respectively the density, the specific heat and the thermal conductivity.

The general form of the heat flux conservation on the boundaries, is given by:

$$q = q_a + q_c + q_r \tag{2}$$

In this relation, q_a is the heat flux determined via Fourier's law:

$$q_a = -(k\nabla T)\vec{n}$$

The term $q_c = h(T - T_{ref})$ describes the heat transferred by convection in the gas that is introduced in the installation. In the above equation, h is the convective heat transfer coefficient and T_{ref} is the reference temperature.

The term q_r is the radiative heat flux, which is given by equation (3). In order to model the radiative heat transfer in our configuration, we have used the "wall to wall" approach employed in FIDAP®. This method is based on the ideal enclosure theory. If the surfaces comprising the enclosure are grey-diffuse, they emit a hemispherical flux proportional to σT^4. So, we consider an enclosure consisting of N grey-diffuse surfaces, which surround a non-participating medium. In this case, the heat exchange between one surface i of the enclosure and all the other radiating surfaces is described by the following law [8]:

$$\sum_{j=1}^{N}\left(\frac{\delta_{ij}}{\varepsilon_j} - F_{ij}\frac{1-\varepsilon_j}{\varepsilon_j}\right)q_r^j = \sum_{j=1}^{N}(\delta_{ij} - F_{ij})\sigma T_j^4 \tag{3}$$

where δ_{ij} is the Kronecker operator, ε_j is the emissivity of the surface j, F_{ij} is the view factor between the surface i and surface j, T_j is the temperature of j'th surface and σ is the Stefan-Boltzmann constant. Equation (3) can be solved after a preliminary calculus of the view factors F_{ij}. Other numerical simulations of the heat transfer by radiation [9-10] indicate that the accuracy of the view factors has a strong influence on the computed temperature field.

The boundary conditions are imposed in such a way, that the temperature of the heating element and the cooling speed are the role parameters that control the simulation. The heat balance through the solid-liquid interface includes the latent heat release.

The energy equation (1) and radiation heat exchange equation (2), are solved by using the finite element method provided by FIDAP® [11]. The solution procedure uses the successive substitution algorithm.

Due to the high non-linearity of equation (2) that contains a term that depends on the fourth power of temperature, the use of relaxation factors is mandatory. The successive substitution algorithm requires relaxation factors between 0.5 and 0.9.

2.2. Results

In the first stage of the simulation, a steady-state result is obtained. This temperature field is used as initial condition for the transient modeling. The time-dependent temperature distribution is analyzed by taking into account the heat transfer by conduction, convection and radiation. From the local temperature profiles in the silicon sample, the shape of the solid-liquid interface, the thermal gradient at the interface (G_L) and the growth rate (V) are evaluated.

The temperature field in the silicon sample is presented in Fig.1. This is characterized by highly curved isotherms, indicating significant radial gradients. It is observed that the thermal gradient in the crystal ($G_S = 1.8\,K/cm$) is greater that the thermal gradient in the melt ($G_L = 0.8\,K/cm$) at the solid-liquid interface. From the transient modeling, average values $G_L \approx 1\,K/cm$ and $V \approx 1\,cm/h$ are obtained.

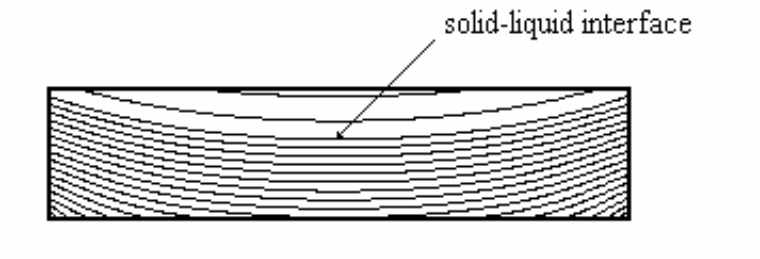

Fig. 1. Thermal field in the silicon sample (temperature difference between two consecutive isotherms $\Delta T = 1.5\,K$).

It is essential to know and control the solidification parameters during all solidification processes because solidification features play a major role in the final product quality. Simulations are powerful tools to calculate and predict the solidification parameters.

In the case of photovoltaic silicon, big grains are required to produce better quality solar cells. Unfortunately, in the range of gradient and growth rate mentioned above, two growth regimes can exist or coexist: columnar grains in the direction of the thermal gradient and equiaxed grains.

Columnar grains are bigger and are thus preferred to equiaxed grains; the last ones deteriorate drastically the quality of photovoltaic silicon. Equiaxed grains grow on seeds in the melt away from interface. The presence of seeds can have two origins: side branches of dendrites are detached from the columnar front and act as seeds or there exists foreign particles in the melt. The detachment of side branches requires that there is a strong convection in the melt, but there does not seem to be the case in this process. On the contrary, the presence of foreign particles in photovoltaic silicon whose raw material often comes from rejected microelectronics silicon is quite. Thus, for this industrial case, we can consider that quiaxed grains mainly nucleate on foreign particles.

Conditions of transition from columnar to equiaxed growth are complex, but a model from J. D. Hunt [12] enables to evaluate the limits of gradient and growth rate for the transition to happen. Figure 2 was calculated by making the assumption that the particles are very efficient for nucleation and, the chemical field ahead of the interface essentially due to carbon. Three domains are delimited

depending on the gradient and growth rate: columnar, columnar plus equiaxed and equiaxed growth. Columnar growth is obtained for high gradients and slow growth rate.

It appears that the point corresponding to the numerical values determined in this paper falls inside the domain of equiaxed growth. In fact, the main point is that, in this range of gradient and growth rate, small changes in the gradient and in the growth rate have a dramatic impact on the solidification features. Consequently, simulations are very important and their results must be as accurate as possible. The work developed here has the great advantage to consider the transient state and so to take into account the latent heat released at the interface upon solidification. However, it is a two dimensional simulation and thus, three-dimensional simulation must be achieved in order to get more accurate results.

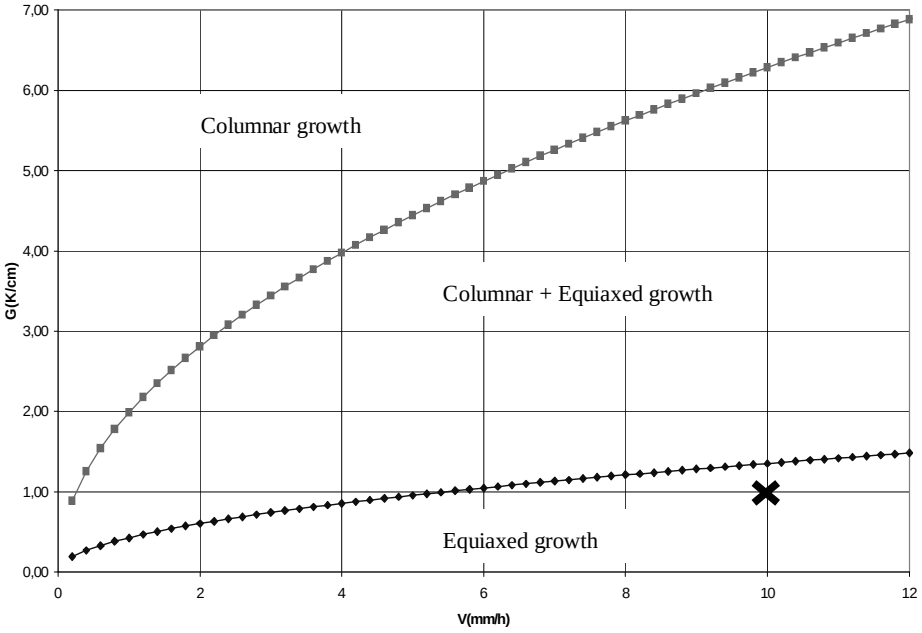

Fig. 2. Domains of different types of growth. The cross corresponds to the results of the transient numerical simulation.

3. 3D steady-state modeling

3.1. Model and mathematics

The 3D square-geometry (see in Fig. 3) considered for the simulation results from several assumptions: (i) the heat transport is slow enough so that a balanced steady-state is computed, i.e. the temperature field does not depends on time for a given geometry of the system, (ii) the under-crucible system (called "tampon") is simplified to one single graphite block which extracts heat form the furnace; (iii) there are no foots under the crucible, but the tampon effective thermal conductivity takes into account their role in heat extraction by conduction; (iv) each of the nine resistive heaters has an uniform temperature, given by its own control thermocouple; (vi) the different stages of the casting process are simulated by building several geometries, with different positions of crucible and/or tampon, regarding to the heater system.

The numerical model is calibrated using experimental measures on thermocouples serving as thermal regulators in the working furnace. This is an important point of the simulation, to be commented in the next paragraph. The silicon growth process takes place in a flow of Ar, a gas with a very small thermal conductivity and transparent to thermal radiation. The melt convection has been neglected in the actual modeling, as well as the gas convection in the whole furnace.

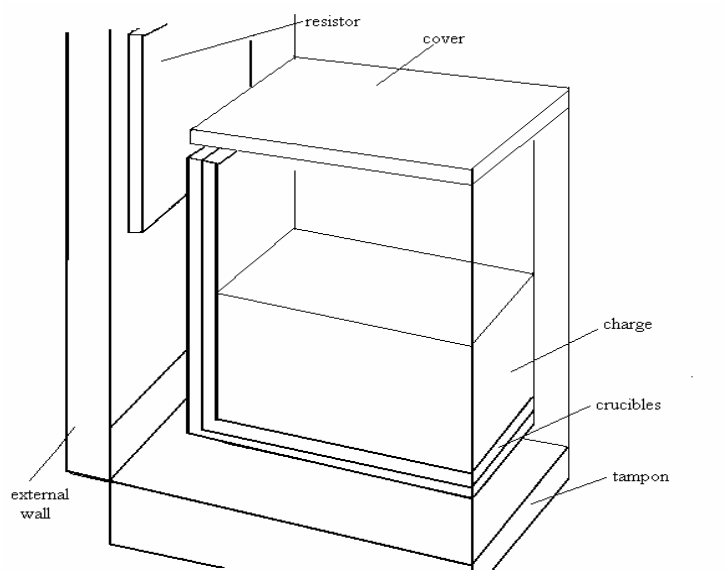

Fig. 3. Detail of the geometrical model (one quarter of the furnace).

In order to obtain the temperature distribution, the whole system is divided in sub-domains. Heat transfer in all sub-domains is described by the steady-state equation:

$$\nabla\left(k\left(T,x,y,z\right)\nabla T\right)+S\left(T,x,y,z\right)=0 \tag{4}$$

where $k(T, x, y, z)$ is the thermal conductivity of the considered domain, and $S(T,x,y,z)$ is a volumetric heat source, generated for example by thermal radiation at the boundaries of the domain corresponding to the gas.

At the solid-liquid interface, i.e. melting point T_M = 1686 K, a change of silicon thermal conductivity takes place.

We have considered the radiation heat transfer in all enclosures of the system because the radiant heat flux, $q_r = \sigma\left(T_{max}^4 - T_{min}^4\right)$, is large compared to the heat transfer rate due to convection or conduction. Fluent provides four radiation models that allow to include radiation in the numerical approaches of the radiation heat transfer: (i) Discrete Ordinates, DO; (ii) Discrete Transfer Radiation Model, DTRM; (iii) P-1; and (iv) Rosseland radiation model [7]. When deciding which radiation approach to use, one consider the value of $\tau = aL$, which represents the optical thickness (depending on a characteristic length, L, and on the absorption coefficient of the substance, a). If $\tau << 1$, the substance is fully transparent, and the DTRM and DO models are appropriate for simulation. If $\tau > 1$, the material is optically thick, and the best models are P-1 and Rosseland .

In the simulation, only the DO method has been employed. According to this model, the radiative transfer equation is solved for a finite number of discrete solid angles, each associated with a vector direction, $\boldsymbol{s}$, fixed in the global Cartesian system (x,y,z).The DO model transforms the radiative transfer equation into a transport equation for radiation intensity in the spatial coordinates (x, y, z). The DO method solves as many transport equations as there are directions $\boldsymbol{s}$. The solution method is identical to that used for the fluid flow and energy equations. The incident radiation heat flux, q_{in}, on a wall surface is calculated and then is used for the net radiation flux from the surface, q_{out}:

$$q_{in} = \int_{\boldsymbol{s}\,\boldsymbol{n}>1} I_{in}\ \boldsymbol{s}\,\boldsymbol{n}\,d\,\Omega \tag{5}$$

$$q_{out} = (1-\varepsilon)q_{in} + n^2\ \varepsilon\ \sigma\ T^4 \tag{6}$$

where n is the refractive index of the medium next to the wall, and ε is the wall emissivity.

Fluent incorporates the radiation flux in the prediction of the wall surface temperature, *T*. Equation (6) also provides the surface boundary condition for the radiation intensity I_0, for all outgoing directions $\boldsymbol{s}$ at the wall, i.e. $I_0 = q_{out}/\pi$.

Symmetry boundary conditions were used, because the physical geometry and the expected pattern of the thermal solution have mirror symmetry. These conditions consist in zero normal gradients of all variables at both symmetry planes.

Calculations were performed by the finite volumes method [7], and focused on the vertical thermal gradient optimization, according to the theory of germination [12]. The computation domains are discretized to obtain a mesh with up to 40000 finite volumes. The number of volumes has been varied from 30000 to 100000 for the whole model, in order to get the thermal field practically unaffected by the mesh density.

3.2. Results

The heat transfer equation has been solved for different tampon positions in the furnace, corresponding to several moments of the casting process. The main parameter of the study was the effective thermal conductivity of the tampon, k_{eff}, computed buy taking into account the extraction of heat through the crucible support. Another result of our study is the estimation of the difference $\Delta T = T_h - T_c$, where T_c is the regulation thermocouple temperature, while T_h is the temperature of the corresponding heater. This could occur because of: (i) thermocouple isolation shield (the thermocouple does not "see directly" the furnace, i.e., there is a thermal resistance between the furnace and the shield); (ii) thermal conduction between shield and external wall; (iii) heat radiation flux exchanged between two-neighboring heater branches. The results of our simulations suggest that the difference between temperature values indicated by a thermocouple and the temperature values of the corresponding heater could be up to ΔT=40 K, as one can see in Fig. 4. Principally, this difference is due to the thermocouple shielding, which prevents thermal exchanges between the regulation thermocouple and corresponding heater, but also realizes a passing bridge between hot and cold zones.

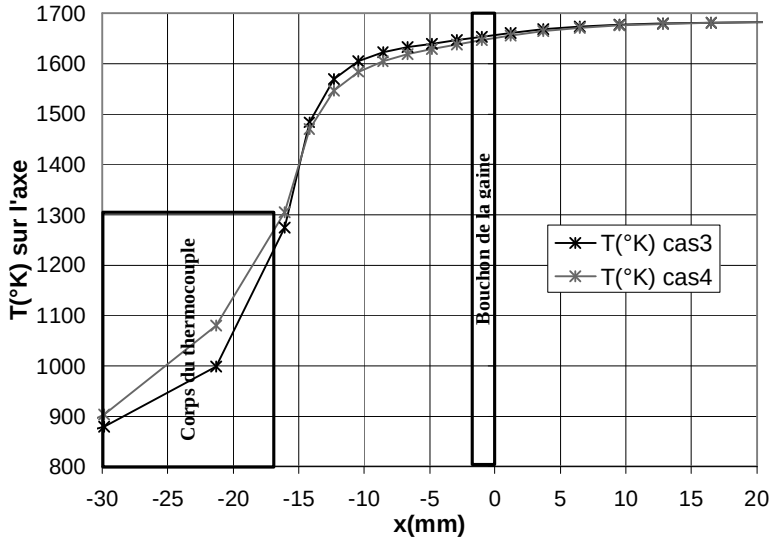

Fig. 4. Calculated temperature distributions along the thermocouple axis, in two cases: cas3- centered thermocouple in its shield; cas4- thermal contact thermocouple-shield.

The vertical thermal gradient in the charge depends on the heat flux extracted in the axial direction of the system. The axial temperature distributions through the system for different k_{eff} values and for different values of ΔT on heaters are shown in Table 1, suggesting that in this system the maximal value of the thermal gradients in the silicon charge does not exceed G_{max}=1.55 K/cm, if the k_{eff} value corresponding to the actual geometry of the supports is only considered. By simulating a tampon having a higher value of its effective thermal conductivity, we assume that the support diameter is increased, that is, the heat extraction is increased in the vertical direction. Consequently, the calculated vertical thermal gradient could be increased.

Table 1. Vertical thermal gradient in the liquid charge for different values of k_{eff} and ΔT.

k_{eff} (W/m K)	ΔT (K)	G (K/cm)
0.85	0	1.45
1.2	20	1.55
1.5	20	1.9
1.5	40	2.1

Vertical thermal gradients values at the inner corners of the crucible are higher than that at the center of the charge, then increasing even more the S-L interface deflection. A comparison between thermal distributions at the center and at the square corner of the charge is shown in Fig. 5. The charge central part is always hotter than its sides.

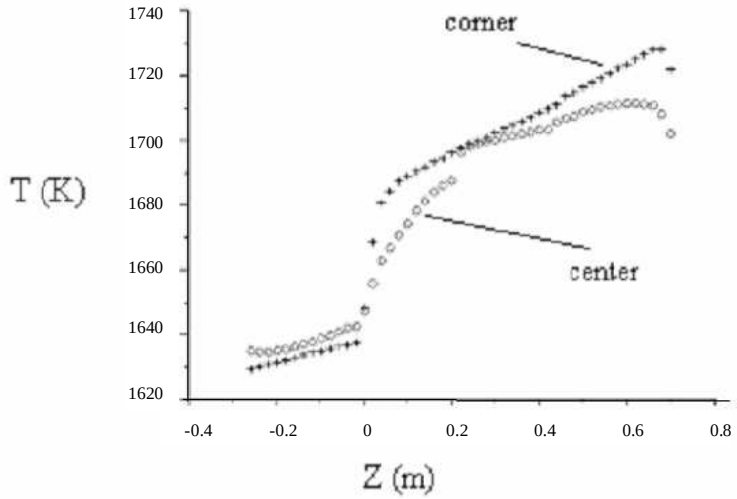

Fig. 5. Axial thermal distributions at the center and at the square corner of the charge.

From these results and by using the model presented in the previous paragraph, it appears that the point corresponding to the numerical values determined in this paper for the highest gradient, i.e. for the conditions where the transition from columnar to equiaxed growth is less favorable, falls inside the domain of mixed columnar and equiaxed growth. So, both 2D and 3D studies confirm that in this domain of solidification conditions the quality of the photovoltaic cells can be deteriorated if the growth conditions are not carefully controlled.

4. Conclusions

An optimum thermal gradient in the charge during the multi-crystalline silicon casting process is difficult to obtain if experimental attempts are only used. The numerical simulation of the solidification process, in a 2D transient and 3D steady state modeling of heat transfer in whole system, were performed taking into account the main physical phenomena.

The results show that the solidification conditions are extreme in this process, in terms of very low growth rates and thermal gradients, essentially due to the huge effect of latent heat release. Compared to a classical columnar-equiaxed transition theory [12], it appears that, in case of pollution of the raw material, equiaxed growth could be obtained, with a detrimental effect on the grain size and consequently, on the cell efficiency. Study is on progress to improve the understanding of grain formation in this system.

The importance of the extraction of heat through the bottom of the furnace is revealed, suggesting that the system is too isolated, in the actual configuration. The effect of the regulation thermocouple isolation shield on the temperature measurements is determined. Resulting differences of about 40 K between heater temperature and thermocouple temperature values were calculated. Comparisons between experimental and computed thermal fields show that the numerical model can be calibrated, by using an appropriate experimental procedure.

Yet, it is essential to consider the transient stage in a 3D configuration taking into account the latent heat released at the interface upon solidification that should reduce the thermal gradient.

The study is still in progress, with the aim to propose optimisation of the technological process, by building a 3D time-dependant model, improving the comprehension of the real furnace and of the grain formation. We are concerned by the relevance of the global numerical modelling to improve the process control of industrial plant. For the design of a new facility, it may be more economical to simulate many possible systems, in order to decide in advance which one is the most promising.

Acknowledgements

The authors would like to thank the company Photowatt Int. S. A. for the technical and financial help provided for this study, especially Dominique Sarti and Christophe Brault.

References

[1] T. Duffar, C. Barat, J. P. Nabot, Material Science and Engineering A **173**, 15-18 (1993).
[2] D. Sarti, R. Einhaus, R. Monna, Q. N. Lê, Matériaux et procédés pour la conversion photo-voltaïque de l'énergie solaire, Séminaire Technique, Sophia Antipolis, France, p.30. 21-21 Nov. 2001.
[3] C. Häßler, G. Stollwerck, W. Koch, W. Krumbe, Proceed.of the 16-th European Photovoltaic Solar Energy Conference, 1-5 May 2000, Glasgow, UK.
[4] F. Barvinschi, T. Duffar, J. L. Santailler, H. Le Gal, J. Crystal Growth **198/199**, 239 (1999).
[5] T. Duffar, "Génie des procèdes de cristallogenèse", Diplôme d'Habilitation à Diriger des Recherches, INPG, CEA, Grenoble, France, 1999.
[6] J. L. Plaza, F. Barvinschi, E. Dieguez, Crystal Research and Technology, **36(7)**, 641 (2001).
[7] Fluent 5.5, Manuals, 2000, Fluent Inc. Illinois, USA.
[8] R. Siegel, J. R. Howell, "Thermal Radiation Heat Transfer", Hemisphere Publishing Corporation, Washington D.C., 1992.
[9] F. Barvinschi, Ph-D Thesis, Institute of Atomic Physics, Bucharest (1998).
[10] K. Lin, P. Dold, Cryst. Res. Technol. **36, 7**, 629 (2001).
[11] FIDAP Manuals, Fluent Inc., Revision 8.0 (1998).
[12] J. D. Hunt, Materials Science & Engineering, **65**, 75 (1984).